Gating at the selectivity filter in cyclic nucleotide-gated channels

Jorge E. Contreras, Deepa Srikumar, and Miguel Holmgren*

Porter Neuroscience Research Center, National Institute of Neurological Disorders and Stroke, National Institutes of Health, Bethesda, MD 20892-3701

Edited by Ramón Latorre, Centro de Estudios Científicos, Valdivia, Chile, and approved December 29, 2007 (received for review October 15, 2007)

By opening and closing the permeation pathway (gating) in response to cGMP binding, cyclic nucleotide-gated (CNG) channels serve key roles in the transduction of visual and olfactory signals. Compiling evidence suggests that the activation gate in CNG channels is not located at the intracellular end of pore, as it has been established for voltage-activated potassium (K_V) channels. Here, we show that ion permeation in CNG channels is tightly regulated at the selectivity filter. By scanning the entire selectivity filter using small cysteine reagents, like cadmium and silver, we observed a state-dependent accessibility pattern consistent with gated access at the middle of the selectivity filter, likely at the corresponding position known to regulate structural changes in KcsA channels in response to low concentrations of permeant ions.

cGMP | ion channel | signal transduction

Cyclic nucleotide-gated (CNG) channels sense variations in the intracellular concentration of cyclic nucleotides that occur in response to visual or olfactory stimuli, therefore playing essential roles in the transduction of visual and olfactory information (1, 2). In many ways, CNG channels are similar to voltage-activated potassium (K_V) channels. They coassemble as tetramers of homologous subunits (3–6), each containing six transmembrane segments (TM), a positively charged TM4 and a reentry P region between TM5 and TM6, suggesting that CNG channels belong to the same superfamily of voltage-activated cation channels (7). The main difference is that CNG channels are only weakly voltage-dependent. Instead, they open and close the pore in response to changes in the intracellular concentrations of cGMP or cAMP, a property conferred by the presence of a cyclic nucleotide binding domain at the C terminus of each subunit (8, 9).

Our understanding of how CNG channels open and close their pore in response to cyclic nucleotide binding is much less refined than our understanding of how K_V channels gate in response to voltage. A large body of evidence, using a variety of approaches, has established that K_V channels open and close their permeation pathway at the intracellular end of the pore (10–17). Attempts to extend those ideas to CNG channels have encountered some resistance. For example, studies using intracellularly applied molecules that block the permeation pathway of CNG channels, such as divalent ions (18), tetracaine (19, 20), or quaternary ammonium ions (21), have shown that blockade is not state-dependent, as if these molecules can access the pore in both open and closed channels, which is in stark contrast with the blockade properties observed in K_V channels (10, 11, 14, 22–24). In addition, experiments examining the state dependence of cysteine modification by intracellular application of methanethiosulfonate (MTS) reagents have failed to show dramatic differences between open and closed states in the inner-vestibule region (21, 25, 26), results that are inconsistent with an intracellular gate in TM6, as shown in K_V channels (12, 15).

Several studies indicate that the pore region of CNG channels plays a role in gating. For example, accessibility of cysteine reagents applied from the intracellular (27, 28) and the extracellular (27–29) side of the channel to cysteines substituted along the entire P region have shown that modification of some residues in this region perturbed normal gating by cGMP. Interestingly, by measuring modification rates in different states of the channel, Liu and Siegelbaum (29) were able to show that the pore helix undergoes conformational changes associated with gating. The pore helix, however, does not line the permeation pathway (13, 30, 31). Hence, the location of the gate remains to be determined.

Recently, the crystal structure of a bacterial nonselective cation channel has been solved (31) and the structure of the P region of this channel has been proposed to be equivalent to that of CNG channels. Using this structure as a model, we introduced cysteines along the selectivity filter as targets for chemical modification with small cysteine reagents like Cd^{2+} and Ag^{+} applied from the intracellular side of the channel. We observe that along the selectivity filter there is a state-dependent pattern consistent with the idea that CNG channels gate at this region, where some positions were readily accessible in the open and closed states, whereas others were accessible in the open state with much slower modification rates in the closed state, similar to observations along the intracellular end of TM6 in K_V channels (12, 15).

Results

Cd^{2+} Accessibility to the Selectivity Filter of CNG Channels. To understand how CNG channels gate, we introduced cysteines along the selectivity filter (Fig. 1) as targets for chemical modification with small cysteine reagents like Cd^{2+} and Ag^{+} (32). Fig. 2*A* shows the experimental protocol used to monitor access of Cd^{2+} to the selectivity filter. Inside-out patches containing many CNG channels were held at 0 mV and subjected to 2 second Cd^{2+} applications either in the absence (closed state) or presence of 2 mM cGMP (open state). The activity of CNG channels before and after each Cd^{2+} treatment was evaluated by subtracting the current in response to brief 50-ms depolarizations to +60 mV in the absence of cGMP from those elicited in the presence of 2 mM cGMP (Fig. 2*A*). As an example, Fig. 2*B* illustrates leak-subtracted cGMP-activated current traces before (black) and after five consecutive Cd^{2+} treatments in the open state to I361C mutant channels (light-brown traces). Cd^{2+} applied from the intracellular face of the membrane produced a complete and irreversible current reduction. For positions I361C (Fig. 2*C*) and T360C (Fig. 2*D*), both located at the inward-facing end of the selectivity filter, Cd^{2+} ions were able to access cysteines in these mutant channels in both open and closed states. In both positions, Cd^{2+} modification occurred more rapidly in the presence of cGMP (open circles) than in the absence of cGMP (filled circles). The reciprocal of the time constant obtained by single-exponential fits of the current

Author contributions: J.E.C. and M.H. designed research; J.E.C. and D.S. performed research; J.E.C. and M.H. analyzed data; and M.H. wrote the paper.

The authors declare no conflict of interest.

This article is a PNAS Direct Submission.

*To whom correspondence should be addressed. E-mail: holmgren@ninds.nih.gov.

This article contains supporting information online at www.pnas.org/cgi/content/full/0709809105/DC1.

www.pnas.org/cgi/doi/10.1073/pnas.0709809105

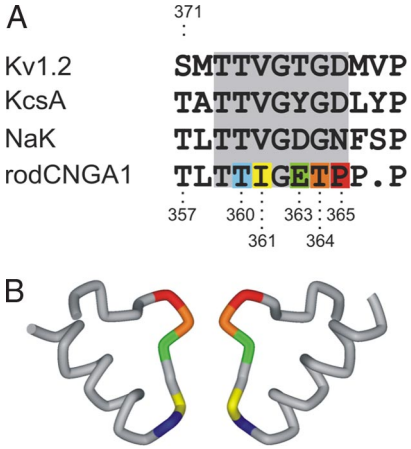

Fig. 1. The selectivity filter of CNG channels. (*A*) Alignment of selectivity filters from various cation-selective channels. Residues that were substituted one at a time by cysteine in CNG channels are highlighted in colors. (*B*) Crystal structure of the P region from NaK channel (31). This bacterial channel allows permeation of Na^+ and K^+, and it is blocked by divalent ions, properties shared by the selectivity filter of CNG channels. Side view of two opposing subunits is shown. Same color pattern as *A*.

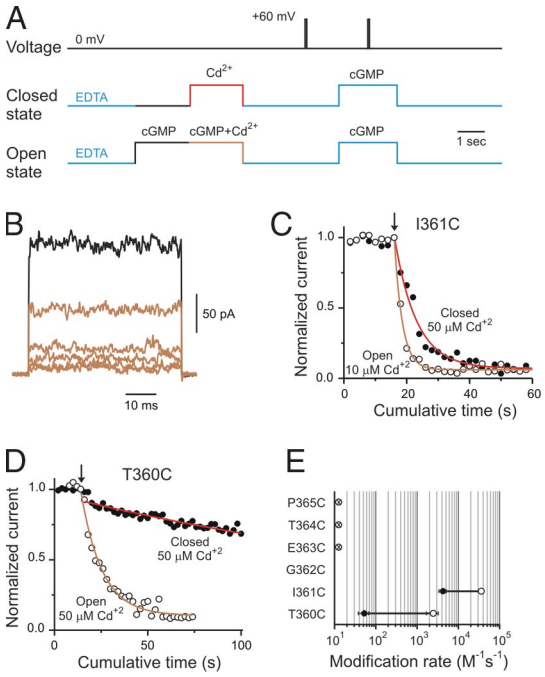

Fig. 2. Cd^{2+} access to the selectivity filter of CNG channels. (*A*) Experimental protocols to assess Cd^{2+} modification in the open and closed states. cGMP-activated currents were monitored by a 50-ms pulse to +60 mV in the presence of 2 mM cGMP. Leak currents were subtracted by a similar pulse performed in the absence of cGMP. Protocols were applied every 15 s. (*B*) cGMP-activated current traces before (black trace) and after five consecutive 10 μM Cd^{2+} treatments (light-brown traces) to I361C mutant channels in the open state. (*C* and *D*) Time courses of the normalized current on Cd^{2+} applications (at arrow) in the open (open circles) and closed (filled circles) states for positions I361C and T360C, respectively. Solid lines represent single-exponential fits to the cumulative modification in the open (light-brown) and closed (red) states. The concentrations of Cd^{2+} used in each experiment are indicated. The best-fit slope values were: 11 s for T360C in the open state, 260 s for T360C in the closed state, 2.5 s for I361C in the open state, and 7 s for I361C in the closed state. (*E*) Accessibility pattern along the selectivity filter. Averages of the modification rates estimated in the open (open circles) and closed (filled circles) states, respectively. Cysteine mutation at position G362 did not render functional channels. Cd^{2+} did not alter cGMP-activated currents in E363C dimer, T364C and P365C mutant channels.

reduction and the $[Cd^{2+}]$ applied were used to estimate the apparent second order modification rates, which are summarized in Fig. 2*E*. The state dependence of Cd^{2+} modification is similar in these positions, with modification rates between 10 to 50 times faster in the open state, suggesting that this end of the selectivity filter experiences conformational changes associated with gating. The current reduction observed at these positions resulted from a direct interaction between the introduced cysteines and Cd^{2+} because similar applications of Cd^{2+} to the background cysteine-less channels did not produce any irreversible alteration in the current levels in either open or closed states [supporting information (SI) Fig. 7]. In contrast, mutant channels containing cysteines at positions expected to be in the lining of the outward-facing end of the selectivity filter (E363C; dimer construct, T364C and P365C), were not modified by Cd^{2+} at 0 mV when the metal was applied from the intracellular side of the membrane, in either the absence or presence of cGMP. Thus, there appears to be a barrier to Cd^{2+} permeation extracellularly to position I361.

Gated Access of Ag^+ to the Selectivity Filter of CNG Channels. We also used Ag^+ to probe accessibility at introduced cysteines in the selectivity filter. This probe has the advantages that it is a monovalent cation, like Na^+ and K^+, ions that permeate at high throughput through CNG channels (33), and it interacts with a single cysteine by covalently modifying the thiolate group (34) rather than requiring the coordination of multiple cysteines as in the case of Cd^{2+}. By using similar experimental protocols (Fig. 3*A*), Ag^+ also produced a complete and irreversible current reduction in T360C and I361C mutant channels (Fig. 3 *B* and *C*). As with Cd^{2+}, Ag^+ was able to modify these mutant channels (Fig. 3*E*) in both open (open circles) and closed states (filled circles), but with much faster modification rates than those measured with Cd^{2+}. For position T360C we observed a small state dependence consistent with the inward-facing end of the selectivity filter undergoing conformational changes associated with gating, similar to the observations when Cd^{2+} was used as a probe. Interestingly, position I361C showed no detectable difference between modification rates determined in open and closed channels, suggesting that the gate in CNG channels should be located more extracellularly than position I361, as suggested by the Cd^{2+} experiments. Ag^+ applied in the presence or absence of cGMP did not alter current levels at position E363C, which is in agreement with the crystal structure of the nonselective cation channel (31), where the side chain of this position is facing away from the ion permeation pathway. Distinctively, Ag^+ applied from the intracellular face of the membrane were able to reach cysteines substituted at position T364C, at the outer end of the selectivity filter, in the open state but to a much lesser extent in closed channels. In the experiment shown in Fig. 3*D*, we first tested access of Ag^+ to closed channels. Six consecutive 10-s Ag^+ treatments had little effect on the activity of T364C channel mutants (Fig. 3*D*, filled circles). However, subsequent 2-s applications in the same patch to open channels produced a fast irreversible current reduction (Fig. 3*D*, open circles). By a single exponential fit to the open-state modification data (brown solid line) we were able to estimate the apparent Ag^+ modification rate to open T364C mutant channels. In addition, the fit provided the maximal degree of the modification, a parameter that was fixed in the fit to the closed-state modification data (Fig. 3*D*, red solid line). Using this approach, we were able to determine that modification rates of cysteines at T364C were ≈250 times faster in the open than in the closed state (Fig. 3*E*). All of these results combined indicate that conformational changes in this region occur as CNG channels open and close in

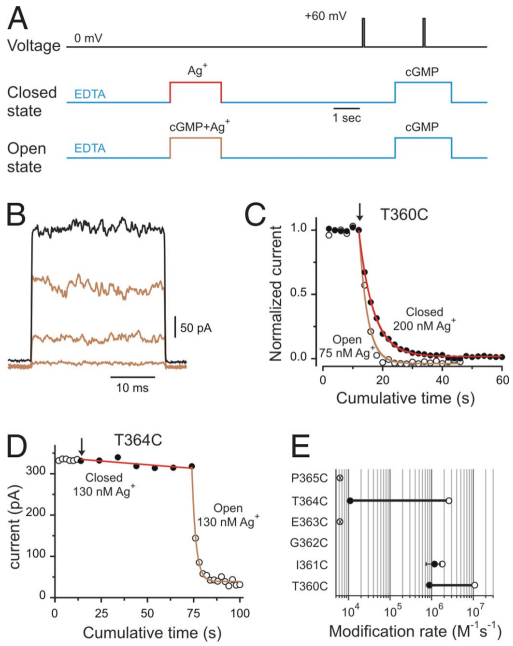

Fig. 3. Ag^+ access to the selectivity filter of CNG channels. (*A*) Experimental protocols to assess Ag^+ modification in the open and closed states. cGMP-activated currents were monitored by a 30-ms pulse to +60 mV in the presence of 2 mM cGMP and leak-subtracted by a similar pulse performed in the absence of cGMP. Protocols were applied every 15 s. (*B*) cGMP-activated current traces before (black trace) and after three consecutive 75 nM Ag^+ applications (light-brown traces) to T360C mutant channels in the open state. (*C*) Time courses of the normalized current on Ag^+ applications (at arrow) in the presence (open circles) and in the absence of cGMP (filled circles) for position T360C. Solid lines represent single-exponential fits to the cumulative modification in the open (light brown) and closed (red) states. The concentrations of Ag^+ used in each experiment are indicated. The best-fit slope values were 2.7 s in the open state and 5 s in the closed state. (*D*) Time course of modification by Ag^+ in T364C mutant channels. Closed (filled circles) and open (open circles) state modifications were assessed in the same patch. Treatments of 130 nM Ag^+ in the closed state were 10 s long. (*E*) Accessibility pattern along the selectivity filter. Averages of the modification rates estimated in the open (open circles) and closed (filled circles) states, respectively. Ag^+ did not alter cGMP-activated currents in E363C dimer and P365C mutant channels.

response to agonist binding, and ions encounter a considerable energetic barrier for permeation somewhere at the middle of the selectivity filter.

To verify that the differences in modification rates at T364C were related to channel gating, we explored how the changes in reactivity correlate with the changes in relative probability of channel opening (P_o). Fig. 4 shows the modification rates normalized to the values obtained at maximal P_o (2 mM cGMP; cyan symbols) together with the levels of relative P_o (red symbols) at different concentrations of cGMP ([cGMP]). Fold changes in modification rates and relative P_o correlate along the entire range of [cGMP], consistent with a simple gated-access mechanism of intracellular Ag^+ to the outward-facing end of the selectivity filter.

Is Ag^+ Using the Selectivity Filter to Reach T364C as It Permeates through CNG Channels?. The pattern of open-channel modification with Ag^+ supports the suggestion that the structure of the selectivity filter from the bacterial nonselective cation channel is a reasonable model of the selectivity filter of CNG channels (31). Crystal structures determined in the presence of divalent ions show unambiguously that divalent ions bind at the external mouth of the selectivity filter (31), which has been functionally reported in CNG channels (35–38). If intracellularly applied Ag^+

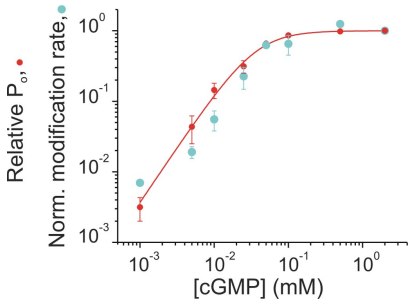

Fig. 4. Gated access to position T364C. Ag^+ apparent modification rates (cyan circles; normalized to the values obtained at 2 mM cGMP) parallel the relative probability of opening (P_o). In each patch ($n = 23$), the relative P_o [red circles; $(I_{[cGMPtest]} - I_{0cGMP})/(I_{2mMcGMP} - I_{0cGMP})$] was estimated before Ag^+ treatments. The solid red line represents a Hill equation fit to the relative P_o data with a slope of 1.6 and a $K_{1/2}$ of 36 μM.

is using the selectivity filter to access position T364C, we should expect that external divalent ions would, by electrostatic and/or steric reasons, interfere with the Ag^+ reaction. Indeed, we observed that the presence of 50 μM extracellular Mg^{2+} in the pipette solution (without divalent chelators) was able to slow the modification rates by Ag^+ in both the open and closed states (Fig. 5 *A* and *B*). This effect of external divalent ions is specific for T364C mutant channels. A similar experiment performed with T360C mutant channels revealed that 100 μM external Mg^{2+} did not change the modification rates at the intracellular end of the selectivity filter (Fig. 5*C*). These data combined suggest that indeed Ag^+ utilizes the selectivity filter to access position T364C.

Access of Ag^+ to the Selectivity Filter of CNG Channels Is Voltage-Dependent. Because intracellular Ag^+ likely accesses position T364C through the selectivity filter, we would expect that the apparent modification rates should be voltage-dependent. Using protocols similar to those shown previously, we determined the modification rates of T364C channels in the open (open symbols) and closed (filled symbols) channels for voltages between −40 and 40 mV (Fig. 6). In open channels, Ag^+ access from the inside seemed to obey the same principles as permeant ions moving through an open pore, where the modification rates at +40 mV are faster than the corresponding rates at −40 mV. At least two factors could contribute to these results. First, there is some intrinsic voltage dependence of gating in CNG channels (39), in which the relative P_o diminishes at negative potentials. Because our experiments were done under saturating [cGMP], this effect

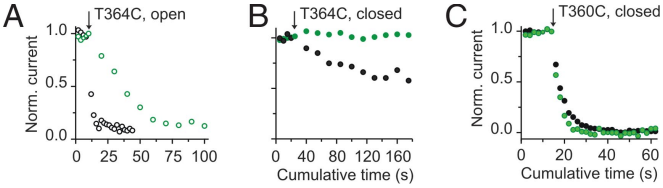

Fig. 5. External divalent ions slow Ag^+ modification rates at the external end of the selectivity filter. (*A*) External Mg^{2+} slows Ag^+ modification of open T364C mutant channels. At arrow, 130 nM Ag^+ treatments were applied either in the absence (black open circles) or in the presence of 50 μM external Mg^{2+} (green open circles). (*B*) External Mg^{2+} prevents Ag^+ modification of closed T364C mutant channels. At arrow, 200 nM Ag^+ treatments of 15 s each were applied either in the absence (black circles) or in the presence of 50 μM external Mg^{2+} (green circles). (*C*) External Mg^{2+} does not prevent Ag^+ modification of closed T360C mutant channels. At arrow, 200 nM Ag^+ treatments of 2 s each were applied either in the absence (black circles) or in the presence of 100 μM external Mg^{2+} (green circles).

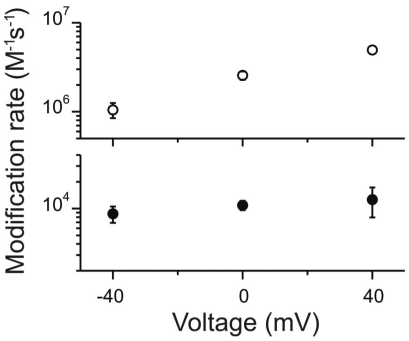

Fig. 6. Voltage dependence of the apparent modification rates at position T364C. Ag^+ apparent modification rates in the open (open circles) and closed (filled circles) states were estimated by using experimental protocols similar to those used in Fig. 3. The concentrations of Ag^+ used in these experiments were between 75 and 130 nM. The ordinate axis was broken between 4×10^4 and 5×10^5, allowing a 20-fold extension of the scales for both open- and closed-state modification data.

is expected to be negligible. Second, the "effective" concentration of Ag^+ at the side chain of position 364 should be equal to $[Ag^+]_{in} \times \exp(z\delta VF/RT)$, where δ is the fractional voltage drop from the intracellular end to the side chain of position 364. Therefore, chemical modification becomes voltage-dependent as the "effective" concentration of Ag^+ at the site of modification changes with voltage. This simple voltage dependence of the apparent modification rates in open channels also suggests that membrane potential does not influence the fraction of reactive thiolate groups at T364C in our experimental conditions.

Intriguingly, the voltage dependence of chemical modification through closed channels did not show the same steepness of the voltage dependence observed with open channels. This implies that voltage-dependent local rearrangements must somehow shape differently the electrostatic potential in the closed state. These results are reminiscent of the state-dependent changes in the electrostatic potential of GluR channels (40). These results further support the notion that Ag^+ uses the selectivity filter to access T364C and the suggestion that gated access in CNG channels occurs at the selectivity filter.

Discussion

Our results indicate that the selectivity filter itself acts as the primary gate in CNG channels. First, we showed a state-dependent gated access of intracellularly applied Ag^+ only to the external end of the selectivity filter, but not to the internal end, suggesting that gating does not arise as a collapse of the entire selectivity filter. Second, the open-to-close ratio for the apparent modification rates with Ag^+ is comparable to similar determinations at the intracellular cavity of K_V channels (12), where the gating mechanism has been established to be a tight closure of the intracellular gate. And third, the apparent modification rates by Ag^+ to T364C satisfactorily follow the relative P_o of the channels, which can be interpreted by a simple gated-access mechanism and not by a more sophisticated kinetic argument as required for inward rectifier K^+ channels (41).

Intuitively, if the gate effectively impedes ion permeation we might have expected a larger open-to-close ratio for Ag^+ modification than those observed here. It is unlikely that modification at position T364C in the absence of cGMP is due to contaminant Ag^+ leaking out through the membrane-glass seal and reaching substituted cysteines from the extracellular environment, because in those experiments the pipette solution contained 10 mM EDTA, which should be sufficient to rapidly chelate any Ag^+ contaminant. Could it be that the P_o in the absence of cGMP is relatively large in T364C mutant channels? Single-channel experiments, like those shown in SI Fig. 8, show that the P_o of T364C mutant channels at +70 mV and in the absence of cGMP is >0.001, similar to determinations performed with the close relative olfactory CNG channels (42). However, the P_o in the absence of cGMP is too low to account for the rates measured in the absence of agonist if modification would have resulted entirely from the access of Ag^+ through open channels. Therefore, these data suggest that the modification of T364C mutant channel at 0 mV in the absence of cGMP arises from Ag^+ permeating through open and also closed channels. Permeation through closed channels has been reported in K_V channels (12, 43). In fact, Ag^+ can squeeze through the intracellular gate in the closed state at apparent rates of $>10^5$ $M^{-1}\,s^{-1}$ (12), which are one order of magnitude faster than those measured at T364C (Fig. 3*E*).

The selectivity filter of K^+ channels has been shown to be a dynamic region. For example, C-type inactivation in K_V channels has been shown to be related to conformational changes at the outer mouth of the selectivity filter (44). Similarly, subconductance states have been related to molecular rearrangements within the selectivity filter of K_V channels (45, 46). Recently, the molecular determinants of inactivation in KcsA have been demonstrated to occur at the selectivity filter (47). In these channels, however, the activation gate that opens and closes the permeation pathway in response to voltage or pH has been established to be at the intracellular end of the last transmembrane segment (10–16, 48–50). In stark contrast, our findings point to the selectivity filter itself acting as the primary gate in CNG channels, which might be a mechanism occurring in other cation channels. Accumulating evidence in Ca^{2+}-activated potassium channels and some inward rectifier potassium channels suggests that the activation gate in these channels is not located at the intracellular end of the last transmembrane segment (51–54). In these channels, however, the role of the selectivity filter in gating remains to be established. Crystal structures of KcsA determined at low permeant ion concentrations revealed a selectivity filter incompatible with permeation (55, 56). One of the conformational changes from a conductive to a nonconductive selectivity filter involves the rotation of the main chain at Gly^{77} to occlude the pore. This dynamic role for Gly^{77} has been shown to be related to its surrogated role as a D-amino acid (57, 58). Interestingly, the equivalent position in CNG channels is G362, a position that cysteine substitution was not permissive, and the region in which the state-dependent access of Ag^+ changed abruptly. Therefore, it is tempting to propose that a similar mechanism might be governing gating in CNG channels in response to agonist.

Materials and Methods

Expression and Constructs of CNG Channels. cDNA of the cysteine less CNGA1 channel was kindly provided by William Zagotta (University of Washington, Seattle). cRNA was synthesized by using a T7 promoter-based *in vitro* synthesis (Ambion), it was injected into *Xenopus* oocytes and recordings were performed 3–5 days after injection. Amino acid substitutions were confirmed by DNA sequencing.

To avoid spontaneous cross-linking of I361C mutant channels (27), substitution H420Q was added to this construct (59). Adenosine at position +4 was mutated to guanine to increase expression levels (60), resulting in a K2E mutation. This mutation does not alter the function of CNG channels. The dimer construct to study E363C was built by standard PCR techniques and it contains a linker constituted by QQQQIEGRQQQQA.

Experimental Solutions. In experiments using Cd^{2+}, the pipette and bath solutions contained (in mM): 120 NaCl, 10 Hepes, and 0.2 mM EDTA (pH 7.4, adjusted with NaOH). When Cd^{2+} was applied to the channels, EDTA was removed from the bath solution. In experiments using Ag^+, the pipette and bath solutions contained (in mM): 120 $NaNO_3$, 10 EDTA, 10 Hepes (pH 7.4). A concentrated stock of $AgNO_3$ in water was prepared freshly for each experiment and protected from the light. The stock was used to prepare bath solution containing a total of 21, 36.75, or 52.5 μM $AgNO_3$. With 10 mM EDTA,

the free Ag^+ concentrations were 75 nM, 130 nM, or 200 nM, respectively. In experiments performed in the presence of extracellular Mg^{2+}, EDTA was removed from the pipette solution. Experiments performed with T364C mutant channels, 50 μM TCEP was added to the pipette solution to avoid spontaneous cross-linking formation (27). Na^+ Salts and $AgNO_3$ (puriss, p.a. grades) were purchased from Fluka. EDTA, cGMP (Na^+ salt), and $CdCl_2$ were obtained from Sigma–Aldrich, and Hepes was acquired from American Bioanalytical.

Currents from inside-out excised patches (61) were recorded by using an Axopatch 200B amplifier (Axon Instruments), sampled at 2.5–10 kHz and low-pass-filtered at 1 or 2 kHz. Patch electrodes with tip diameter between 8 and 15 μm were made with borosilicate glass pipettes. Macroscopic data analysis was performed with pClamp 9 (Axon Instruments) and Origin 7 (Microcal Software) software. Solutions were switched by a computer-controlled rapid solution changer (RSC-200; Biologic Science Instruments).

ACKNOWLEDGMENTS. We thank Dr. William Zagotta for kindly providing the CNGA1 cysteine-less construct. We thank Kenton Swartz, Shai Silberberg, and Holmgren lab members for helpful discussions, and the DNA-sequencing facility of the National Institute of Neurological Disorders and Stroke (NINDS) for sequencing all DNA constructs. J.E.C. is supported by a Ruth L. Kirschstein Postdoctoral Fellowship. This work was supported by the Intramural Research Program of the National Institutes of Health, National Institute of Neurological Disorders and Stroke.

1. Stryer L (1986) *Annu Rev Neurosci* 9:87–119.
2. Zufall F, Firestein S, Shepherd GM (1994) *Annu Rev Biophys Biomol Struct* 23:577–607.
3. Weitz D, Ficek N, Kremmer E, Bauer PJ, Kaupp UB (2002) *Neuron* 36:881–889.
4. Zheng J, Trudeau MC, Zagotta WN (2002) *Neuron* 36:891–896.
5. Zheng J, Zagotta WN (2004) *Neuron* 42:411–421.
6. Zhong H, Molday LL, Molday RS, Yau KW (2002) *Nature* 420:193–198.
7. Jan LY, Jan YN (1990) *Nature* 345:672.
8. Kaupp UB, Seifert R (2002) *Physiol Rev* 82:769–824.
9. Zagotta WN, Siegelbaum SA (1996) *Annu Rev Neurosci* 19:235–263.
10. Armstrong CM (1971) *J Gen Physiol* 58:413–437.
11. Armstrong CM, Hille B (1972) *J Gen Physiol* 59:388–400.
12. del Camino D, Yellen G (2001) *Neuron* 32:649–656.
13. Doyle DA, Morais Cabral J, Pfuetzner RA, Kuo A, Gulbis JM, Cohen SL, Chait BT, MacKinnon R (1998) *Science* 280:69–77.
14. Holmgren M, Smith PL, Yellen G (1997) *J Gen Physiol* 109:527–535.
15. Liu Y, Holmgren M, Jurman ME, Yellen G (1997) *Neuron* 19:175–184.
16. Perozo E, Cortes DM, Cuello LG (1999) *Science* 285:73–78.
17. Jiang Y, Lee A, Chen J, Cadene M, Chait BT, MacKinnon R (2002) *Nature* 417:523–526.
18. Karpen JW, Brown RL, Stryer L, Baylor DA (1993) *J Gen Physiol* 101:1–25.
19. Fodor AA, Black KD, Zagotta WN (1997) *J Gen Physiol* 110:591–600.
20. Fodor AA, Gordon SE, Zagotta WN (1997) *J Gen Physiol* 109:3–14.
21. Contreras JE, Holmgren M (2006) *J Gen Physiol* 127:481–494.
22. Armstrong CM (1966) *J Gen Physiol* 50:491–503.
23. Armstrong CM (1969) *J Gen Physiol* 54:553–575.
24. Choi KL, Mossman C, Aube J, Yellen G (1993) *Neuron* 10:533–541.
25. Flynn GE, Zagotta WN (2001) *Neuron* 30:689–698.
26. Sun ZP, Akabas MH, Goulding EH, Karlin A, Siegelbaum SA (1996) *Neuron* 16:141–149.
27. Becchetti A, Gamel K, Torre V (1999) *J Gen Physiol* 114:377–392.
28. Becchetti A, Roncaglia P (2000) *Pflügers Arch* 440:556–565.
29. Liu J, Siegelbaum SA (2000) *Neuron* 28:899–909.
30. Long SB, Campbell EB, Mackinnon R (2005) *Science* 309:897–903.
31. Shi N, Ye S, Alam A, Chen L, Jiang Y (2006) *Nature* 440:570–574.
32. Lu Q, Miller C (1995) *Science* 268:304–307.
33. Fesenko EE, Kolesnikov SS, Lyubarsky AL (1985) *Nature* 313:310–313.
34. Dance IG (1986) *Polyhedron* 5:1037–1104.
35. Eismann E, Muller F, Heinemann SH, Kaupp UB (1994) *Proc Natl Acad Sci USA* 91:1109–1113.
36. Gavazzo P, Picco C, Eismann E, Kaupp UB, Menini A (2000) *J Gen Physiol* 116:311–326.
37. Park CS, MacKinnon R (1995) *Biochemistry* 34:13328–13333.
38. Root MJ, MacKinnon R (1993) *Neuron* 11:459–466.
39. Benndorf K, Koopmann R, Eismann E, Kaupp UB (1999) *J Gen Physiol* 114:477–490.
40. Sobolevsky AI, Yelshansky MV, Wollmuth LP (2005) *Biophys J* 88:235–242.
41. Phillips LR, Enkvetchakul D, Nichols CG (2003) *Neuron* 37:953–962.
42. Nache V, Schulz E, Zimmer T, Kusch J, Biskup C, Koopmann R, Hagen V, Benndorf K (2005) *J Physiol* 569:91–102.
43. Soler-Llavina GJ, Holmgren M, Swartz KJ (2003) *Neuron* 38:61–67.
44. Liu Y, Jurman ME, Yellen G (1996) *Neuron* 16:859–867.
45. Chapman ML, VanDongen AM (2005) *J Gen Physiol* 126:87–103.
46. Zheng J, Sigworth FJ (1997) *J Gen Physiol* 110:101–117.
47. Cordero-Morales JF, Cuello LG, Zhao Y, Jogini V, Cortes DM, Roux B, Perozo E (2006) *Nat Struct Mol Biol* 13:311–318.
48. Heginbotham L, LeMasurier M, Kolmakova-Partensky L, Miller C (1999) *J Gen Physiol* 114:551–560.
49. Kelly BL, Gross A (2003) *Nat Struct Biol* 10:280–284.
50. Blunck R, Cordero-Morales JF, Cuello LG, Perozo E, Bezanilla F (2006) *J Gen Physiol* 128:569–581.
51. Bruening-Wright A, Schumacher MA, Adelman JP, Maylie J (2002) *J Neurosci* 22:6499–6506.
52. Klein H, Garneau L, Banderali U, Simoes M, Parent L, Sauve R (2007) *J Gen Physiol* 129:299–315.
53. Wilkens CM, Aldrich RW (2006) *J Gen Physiol* 128:347–364.
54. Xiao J, Zhen XG, Yang J (2003) *Nat Neurosci* 6:811–818.
55. Zhou Y, MacKinnon R (2003) *J Mol Biol* 333:965–975.
56. Zhou Y, Morais-Cabral JH, Kaufman A, MacKinnon R (2001) *Nature* 414:43–48.
57. Valiyaveetil FI, Leonetti M, Muir TW, Mackinnon R (2006) *Science* 314:1004–1007.
58. Valiyaveetil FI, Sekedat M, Mackinnon R, Muir TW (2004) *Proc Natl Acad Sci USA* 101:17045–17049.
59. Gordon SE, Zagotta WN (1995) *Neuron* 14:177–183.
60. Kozak M (1997) *EMBO J* 16:2482–2492.
61. Hamill OP, Marty A, Neher E, Sakmann B, Sigworth FJ (1981) *Pflügers Arch* 391:85–100.